

sodium hyaluronate polysaccharide and sample length [19], which allows one to control the nonlinear-optical parameters of the material itself and functional elements based on it.

5. Conclusion

The studies considered above have shown that the combination of proteins and polysaccharides created by Nature and self-organized with silicon dioxide extracted from sea water under natural conditions produced a unique nonlinear-optical biomineral nanocomposite material combining the flexibility and strength of a protein with the elasticity and strength of silicon dioxide, which is promising for applications in photonics. This process can be reproduced under artificial conditions using the adaptable sol-gel technology, which opens up a broad perspective for manufacturing new passive and active optoelectronic devices.

References

1. Churyumov G I, Maksimov I S, Ust'yantsev M A *Usp. Sovrem. Radioelektron.* (11) 35 (2005)
2. Meyers M A et al. *Prog. Mater. Sci.* **53** 1 (2008)
3. Müller W E G et al. *Biosensors Bioelectron.* **21** 1149 (2006)
4. Leys S P, Mackie G O, Reisswig H M *Adv. Marine Biol.* **52** 1 (2007)
5. Kulchin Yu N et al. *Vestn. Dal'nevost. Otd. Ross. Akad. Nauk* (1) 27 (2007)
6. Kulchin Yu N et al. *Opt. Memory Neural Networks* **16** 189 (2007)
7. Kulchin Yu N et al. *Kvantovaya Elektron.* **38** 51 (2008) [*Quantum Electron.* **38** 51 (2008)]
8. Galkina A N et al. *Khim. Fiz. Mezoskop.* **11** 310 (2009)
9. Voznesenskii S S et al. *Ross. Nanotekhnol.* **5** (1–2) 126 (2010) [*Nanotechnol. Russia* **5** (1–2) 142 (2010)]
10. Kulchin Yu N *Rare Met.* **28** (Special issue) 66 (2009)
11. Aizenberg J et al. *Proc. Natl. Acad. Sci. USA* **101** 3358 (2004)
12. Kul'chin Yu N et al. *Pis'ma Zh. Tekh. Fiz.* **34** (15) 1 (2008) [*Tech. Phys. Lett.* **34** 633 (2008)]
13. Kulchin Yu N et al. *Fotonika Biomineral'nykh i Biomimeticheskikh Struktur i Materialov* (Photonics of Biomineral and Biomimetic Structures and Materials) (Moscow: Fizmatlit, 2011)
14. Konorov S O et al. *Zh. Eksp. Teor. Fiz.* **123** 975 (2003) [*JETP* **96** 857 (2003)]
15. Kul'chin Yu N et al. *Opt. Spektrosk.* **107** 468 (2009) [*Opt. Spectrosc.* **107** 442 (2009)]
16. Maslov D V, Ostroumov E E, Fadeev V V *Kvantovaya Elektron.* **36** 163 (2006) [*Quantum Electron.* **36** 163 (2006)]
17. Agrawal G P *Nonlinear Fiber Optics* (San Diego: Academic Press, 1995) [Translated into Russian (Moscow: Mir, 1996)]
18. Kulchin Yu N et al., in *Biosilica in Evolution, Morphogenesis, and Nanobiotechnology* (Eds W E G Müller, M A Grachev) (Berlin: Springer, 2009) p. 315
19. Kulchin Yu N et al. *Laser Phys.* **21** 630 (2011)
20. Dunn B et al. *Acta Mater.* **46** 737 (1998)
21. Shchipunov Yu A, in *Perspektivnye Napravleniya Razvitiya Nanotekhnologii v DVO RAN* (Promising Directions in the Development of Nanotechnologies at the Far Eastern Branch, Russian Academy of Sciences) Vol. 2 (Executive Ed. Yu N Kulchin) (Vladivostok: Dal'nauka, 2009) p. 157

PACS numbers: 37.10.De, 37.10.Gh, 32.30.Jc
DOI: 10.3367/UFNe.0181.201108j.0896

Laser cooling of rare-earth atoms and precision measurements

N N Kolachevsky

1. Introduction

Today, the physics of microwave and optical frequency standards is one of the most rapidly advancing lines of inquiry. Progress here can be readily quantitatively evaluated: while in the early 2000s the problem of reaching a measurement inaccuracy at a level of 10^{-15} was considered [1], now systems capable of generating highly stable signals with a fractional inaccuracy better than 10^{-17} are being developed [2].

The improvement in frequency stability opens new possibilities for solving problems of time and frequency metrology, global positioning and navigation, geodesy, gravimetry, and the sensitive testing of fundamental physical theories. The solution to these problems at the modern level of precision requires the practical realization of new principles of generating time and frequency signals on Earth surface and in space. In 2014, the orbital launching of ACES (Atomic Clock Ensemble in Space) is planned, which constitutes an ensemble of high-precision microwave atomic clocks with an inaccuracy of a few digits in the 16th decimal place [3]. Simultaneously, methods are being developed for transmitting extremely stable signals via both conventional microwave channels and optical communication lines [4]. Precise time and frequency signals are required in numerous fundamental and applied problems, making this research field one of the most urgent issues in modern physics.

A considerable improvement in the accuracy of frequency standards has been achieved mainly due to advances in the development of optical clocks operating in the frequency range close to $\nu_0 \sim 10^{15}$ Hz. The increase in the carrier frequency compared to microwave standards ($\nu_0 \sim 10^{10}$ Hz) for the same spectral linewidth $\delta\nu$ has led to an increase in the resonance quality factor $Q = \nu_0/\delta\nu$ and a corresponding decrease in the inaccuracy. To excite and detect narrow optical transitions (the typical width today is $\delta\nu \sim 1$ Hz), it is necessary to solve a number of problems: (i) to create stable laser systems emitting lines with spectral widths smaller than 1 Hz; (ii) to search for optimal atomic and ion systems providing the best metrological characteristics, and (iii) to develop methods for cooling atoms and for exciting and interrogating resonances providing the ultimate accuracy.

Recent advances in the stabilization of lasers have proved to be so significant (see review [5]) that these light sources have become a reliable tool accessible to any laboratory in the

N N Kolachevsky Lebedev Physical Institute, Russian Academy of Sciences, Moscow, Russian Federation;
Moscow Institute of Physics and Technology (State University),
Dolgoprudnyi, Moscow region, Russian Federation
E-mail: kolik@lebedev.ru

Uspekhi Fizicheskikh Nauk **181** (8) 896–903 (2011)
DOI: 10.3367/UFNr.0181.201108j.0896
Translated by M Sapozhnikov; edited by A Radzig

world. At the same time, the question of the choice of optimal metrological transitions remains open to a certain degree, and now quite different atomic systems and different interrogation methods are being extensively investigated. We shall exemplify clocks based on single ions [2], which offer the indisputable advantage of the almost perfect isolation of ions from external interactions, and optical lattice clocks based on neutral atoms [6], which provide high long- and mid-term stability due to the large number of interrogated atoms.

In this report, rare-earth atoms with the open 4f electron shell (such as Pr, Nd, Dy, Er, Tm) are discussed as potential candidates for use in optical clocks. To create an optical clock, it is necessary to resolve the following issues: to provide a low temperature of atoms, to isolate them from the environment, and to provide a long interaction time with the exciting laser field. These problems are gotten around using the laser cooling method, its applicability to a certain atom requiring a separate careful study. In 2009, the laser cooling of a thulium atom was demonstrated for the first time at the Laboratory of Optics of Active Media at the Lebedev Physical Institute, RAS (FIAN in *Russ. abbr.*). The report presents the review of recent results obtained by researchers at the FIAN laboratory and by students and postgraduates at the Moscow Institute of Physics and Technology (MIPT).

The paper outline is as follows. The possibility of utilizing the intrashell magnetic dipole 4f–4f transitions in a thulium atom for optical frequency standards is analyzed in Section 2. In Section 3, the review of basic results on the laser cooling of thulium and its magneto-optical trapping is presented. Section 4 is devoted to the study of the sub-Doppler cooling of thulium and its magnetic dipole trapping.

2. Transitions between fine-structure sublevels of a ground-state thulium atom

A specific feature of the ground state of rare-earth atoms with the open 4f shell is the presence of the fine structure: depending on the quantum number of the total electron momentum J , determined by the mutual orientation of electron momenta in the 4f shell, the ground state is split into a number of fine-structure sublevels. In this case, the 4f shell is located inside the closed outer 5s² and 6s² shells, providing the screening of fine-structure sublevels by outer shell electrons.

In 1986, Aleksandrov et al. [7] pointed out for the first time the possibility of employing optical transitions between the ground-state fine-structure components as metrological transitions because the electron screening considerably reduces the sensitivity to atomic collisions with a buffer gas. Later on, the screening in collisions with He atoms was quantitatively examined in experiments [8] and confirmed by calculations [9, 10]. As this takes place, the ratio of elastic and inelastic collision cross sections for ground-state Tm atoms is of order 5×10^4 (see paper [10] and references cited therein).

In 1999, it was proposed at the Laboratory of Optics of Active Media (FIAN) to use the magnetic dipole $4f^{13}6s^2 (J = 7/2) \rightarrow 4f^{13}6s^2 (J = 5/2)$ transition in a thulium atom at a wavelength of 1.14 μm with a spectral width of 1.1 Hz (see Fig. 1) as a promising candidate for optical clocks (some parameters of this transition are presented in paper [11]). This idea was supported by I I Sobel'man and the study of rare-earth atoms was initiated at the Laboratory. First, it was assumed that in the presence of screening it is appropriate to excite the metrological transition in a dense

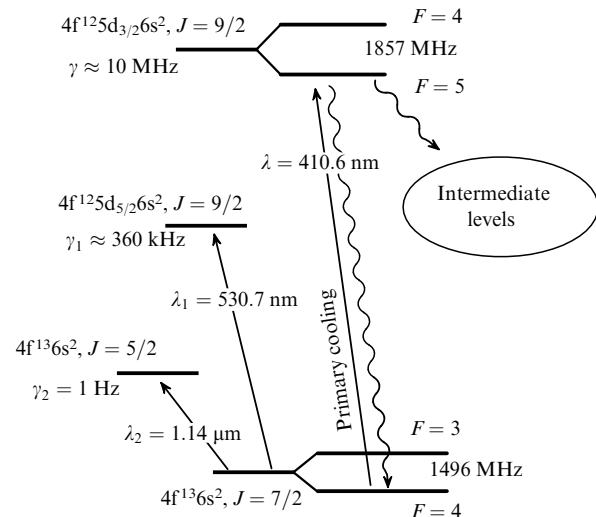


Figure 1. Energy level diagram of the ^{169}Tm atom. Shown are the ground-state fine structure (the $4f^{13}6s^2$ configuration), hyperfine-structure components, and atomic energy levels used for the primary and secondary laser cooling at wavelengths of 410.6 and 530.7 nm, respectively.

laser-cooled cloud of thulium atoms, which can provide the high short-term stability of a standard. However, in 2010 researchers at Harvard University (USA) found in experiments that the screening effect disappeared in collisions between Tm atoms in certain spin states [12], which complicates the construction of an optical clock based on a dense atomic cloud.

More promising is an idea underlying the estimate of the differential polarizability of the $J = 7/2$ and $J = 5/2$ ground-state levels in thulium [13]. The scalar polarizability of the $J = 7/2$ ground state of thulium is $\alpha_s = 161$ atomic units (a.e.) [9] and is comparable with the polarizability of the ground state, for example, of rubidium (319 a.e.). The analysis of the fine structure of a thulium atom points to the fact that polarizabilities for the $J = 7/2$ and $J = 5/2$ fine-structure components in the ground state should be close: allowed transitions from each of the ground-state sublevels $4f^{13}6s^2 (J = 7/2)$ and $4f^{13}6s^2 (J = 5/2)$ have close wavelengths and oscillator strengths. The structure of even terms in thulium is split into two virtually identical branches separated by an interval of about 8800 cm^{-1} , corresponding to the ground-state fine splitting. Each of the branches has its own ionization threshold. The allowed transitions from the odd $4f^{13}6s^2 (J = 7/2)$ and $4f^{13}6s^2 (J = 5/2)$ levels to the corresponding components of these branches are also identical to a great extent, resulting in the identical polarizabilities of the ground-state levels.

The detailed calculation of the differential polarizability is time-consuming [13] and has not been performed to date. However, if we admit that the assumption of a low differential polarizability is correct, a new outlook opens for using the 1.14- μm magnetic dipole transition in optical clocks.

One of the possibilities resides in the localization of thulium atoms in the antinodes or nodes of a standing light wave (optical lattice), as is realized in optical clocks based on strontium and ytterbium atoms (see, for example, paper [6] and references cited therein). In this case, the contribution of the Doppler effect is suppressed (the Lamb–Dicke regime) and the interaction between atoms is eliminated. However, it is necessary to take into account the dynamic Stark shift

caused by the optical lattice itself. In the case of Sr, the wavelength of the optical lattice is carefully selected, so that the dynamic Stark shifts of the upper and lower metrological levels would be the same (the ‘magic’ wavelength [14]). For the 1.14- μm transition in a thulium atom, any wavelength will be in fact ‘magic’, because the polarizabilities of the levels are identical. This considerably alleviates the problem of loading atoms into the lattice and allows one to work in a convenient spectral range.

Another important consequence can be suppression of the frequency shift caused by the black body radiation. Today, it is this effect that mainly restricts the accuracy of optical lattice clocks based on Sr atoms [15]. Because this effect is simply reduced to the dynamic Stark shift caused by broadband radiation of heated surrounding bodies, the coincidence of polarizabilities of metrological levels will result in its suppression.

So far, direct precision spectroscopy of magnetic dipole transitions between the fine-structure sublevels in ground-state rare-earth atoms has not been performed. The problems discussed in this section require the experimental verification and detailed quantitative estimate. We assume that the 1.14- μm magnetic dipole transition of a thulium atom is not inferior in its basic metrological characteristics to clock transitions in Sr and Yb atoms, which have found wide applications in optical clocks with a fractional inaccuracy of order 10^{-16} .

In turn, to perform precision measurements and to load atoms into optical traps, temperatures lower than 10 μK are required, which can be achieved only by the laser cooling method. In our country, laser cooling is being actively studied by research groups at the Institute of Spectroscopy, RAS, where cold rubidium atoms are investigated [16]; at the Institute of Laser Physics, SB RAS, where the use of laser-cooled magnesium atoms for frequency standard problems is planned [17]; at the Institute of Semiconductor Physics, RAS, where cold Rydberg rubidium atoms are studied [18]; at the Institute of Applied Physics, RAS, where the two-dimensional lithium Fermi condensate was produced [19], and at the All-Russian Research Institute of Physicotechnical and Radio Engineering Measurements, where several cesium fountains are working [20] and an optical clock built around Sr atoms is being developed. In Section 3, the original results of studies on the laser cooling of thulium atoms, pursued at FIAN, are presented.

3. Magneto-optical trap for thulium atoms

3.1 Laser cooling of new atomic ensembles

The laser cooling method opened fundamentally new possibilities in the fields of precision laser spectroscopy [21], the investigation of particle collisions [22], atomic interferometry, and the production of quantum condensates [23]. This method is not universal because the efficient laser cooling of an atom can be achieved if the following requirements are fulfilled: (i) the atom should have a cyclic transition in the optical (UV) spectral range; (ii) the transition should be strong enough (the transition probability $A \sim 10^8 \text{ s}^{-1}$) to provide the high cooling rate, and (iii) a laser with high enough power ($P \sim 1 \text{ mW}$), being tuned to resonance with this transition, is needed.

At present, laser cooling and trapping in magneto-optical traps (MOTs) have been achieved for all alkali and alkali-

earth atoms, as well as metastable-state noble gas atoms (except for radon). The possibility of laser cooling and trapping of atoms from the rest of the Periodic Table is being extensively investigated. In recent years, the laser cooling and trapping of the Hg [24], Cd [25], and some other atoms in MOTs have been demonstrated. The use of new ultracold atomic ensembles is planned for solving problems in metrology, quantum informatics, investigations of particle collisions, and testing fundamental physical theories. For example, an important unsolved problem is the efficient laser cooling of hydrogen (antihydrogen) atoms, which will allow one to compare the spectra of matter and antimatter with a high resolution and perform sensitive tests of the *CPT* theorem. This problem became even more urgent after the successful synthesis and trapping of antihydrogen atoms in a magnetic trap [26].

Aside from the metrological applications discussed in Section 2, laser-cooled rare-earth atoms are of great interest for the problems of quantum condensates and studies of molecular structures. The magnetic moment of these atoms in the ground state is many times higher than that of alkali atoms. This moment for a Tm atom is $4\mu_B$, and for Dy, for example, amounts to $10\mu_B$ (μ_B is the Bohr magneton), which opens wide possibilities for studying the magnetic interactions of atoms with superconductors [27] and dipole-dipole interactions [28]. The possibility has appeared of synthesizing cold polar molecules [29] having a magnetic moment (for example, TmRb).

In the last few years, the laser cooling of the two representatives of rare-earth elements with an open 4f shell, erbium [30] and dysprosium [31], has been achieved in the USA. In turn, in our laboratory at FIAN we have demonstrated the laser cooling of thulium atoms [32, 33]. The laser cooling of rare-earth atoms is complicated due to the absence of strong cyclic transitions from the ground state. Because of a great number of intermediate energy levels, there always exists a probability of depopulation from the cooling cycle, which cannot be ‘shut off’ by repumping lasers, as, for example, in rubidium. The calculation of transition probabilities in these atoms is rather inaccurate and can give only rough estimates of the decay probability.

3.2 Cooling and magneto-optical trapping of thulium atoms

Earlier, we investigated optical transitions in a thulium atom convenient for laser cooling [11]. Thulium possesses the only stable isotope ^{169}Tm with the nuclear spin $I = 1/2$ (bosonic isotope). Therefore, each its energy level will be split into two hyperfine-structure sublevels. It was proposed to utilize the strong, almost cyclic $4f^{13}6s^2$ ($J = 7/2$, $F = 4$) \rightarrow $4f^{12}5d6s^2$ ($J = 9/2$, $F = 5$) transition at 410.6 nm with the natural width $\gamma = 10.0(4) \text{ MHz}$ (see Fig. 1). Here, F is the quantum number of the total atomic moment. Despite the decay of the upper cooling level to intermediate energy levels of the opposite parity (indicated in Fig. 1 as ‘intermediate levels’), in 2009 we managed to demonstrate the efficient Zeeman cooling of a hot Tm atomic beam [32].

A schematic of a setup for laser cooling and magneto-optical trapping of thulium atoms is depicted in Fig. 2. A magneto-optical trap represents a classical setup of three pairs of mutually orthogonal circularly polarized cooling laser beams emitting at frequencies tuned to the red region of the spectrum with respect to the atomic optical transition. The atoms are trapped in a stainless steel vacuum chamber

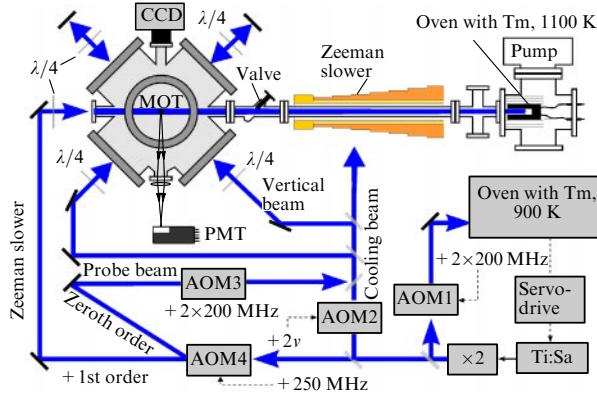


Figure 2. Schematic of the setup for laser cooling of thulium atoms: AOM—acoustooptic modulator; PMT—photomultiplier, and CCD—charge-coupled device.

with optical windows for three orthogonal axes for cooling beams and two additional axes at an angle of 45° for loading and detecting. The chamber is evacuated down to less than 10^{-8} mbar with an ion-getter pump 30 l s^{-1} in capacity. At the center of the chamber, a quadrupole magnetic field on the order of 10 G cm^{-1} is produced with the help of coils in the anti-Helmholtz configuration. The laboratory magnetic field is compensated for by additional coils.

We used in experiments the second harmonic of a cw Ti:sapphire laser at a wavelength of 410.6 nm . The laser frequency was stabilized by a saturated absorption signal generated in the second oven with thulium vapor at 900 K [11]. The second-harmonic frequency was shifted in several acoustooptic modulators to produce three light fields at different frequencies: (1) a light field for a Zeeman slower with frequency detuned by -150 MHz with respect to the frequency of the $F = 4 \rightarrow F = 5$ cooling transition (see Fig. 1); (2) a cooling field with the frequency detuning from the resonance variable in the range from -0.5γ to -4γ , and (3) a probe field tuned exactly to resonance with the cooling transition. A computer-aided digital controller was used to generate pulse trains for all three light fields.

Thulium atoms were loaded from a beam formed in a sapphire oven heated to 1100 K using a system of apertures. This temperature is considerably lower than the thulium melting point (1818 K). However, the metal is efficiently sublimated from a surface, the pressure of saturated thulium vapor at 1100 K being 10^{-2} mbar. The oven volume is evacuated with a turbomolecular pump (30 l s^{-1}) down to 10^{-7} mbar.

The atomic beam was decelerated by a counter light field in a Zeeman slower 40 cm in length producing a longitudinally inhomogeneous magnetic field compensating for the Doppler shift changing during the deceleration of atoms. It was shown in paper [32] that the slower decelerates $\sim 1\%$ of the atoms entering the main chamber to a velocity of 25 m s^{-1} . The velocity distribution of atoms with the switched-off field of the cooler and the low-velocity part of the distribution for the switched-on slower are presented in Fig. 3. In this case, we detected the luminescence signal of atoms excited by the laser field at an angle of 45° to the atomic beam direction. The measurement was performed with a PMT by scanning the probe laser beam frequency, which was followed by the recovery of the atomic velocity distribution. Estimates show that the flux of cold ions at the central part of the vacuum

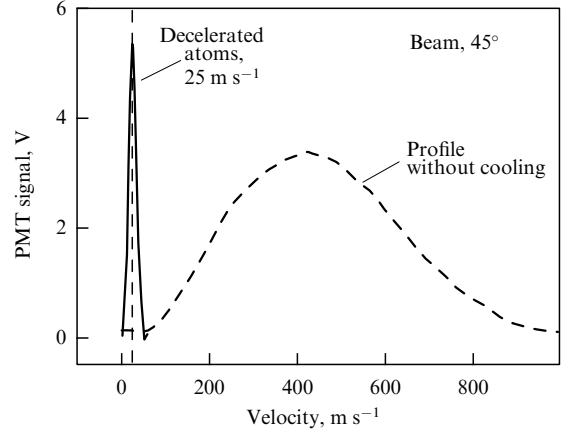


Figure 3. Illustration of the operation of a Zeeman slower for an atomic thulium beam. The dashed curve fits the velocity distribution of thulium atoms for the switched-off moderator. The distribution corresponds to temperature 1100 K . The solid curve is the low-velocity part of the distribution for the operating moderator.

chamber is $10^7 \text{ s}^{-1} \text{ cm}^{-2}$ and has a cross section of about 1 cm^2 .

3.3 Lifetime of atoms in a magneto-optical trap

A cloud of cooled atoms produced in the intersection region of cooling beams had a regular shape, a Gaussian distribution of the luminescence intensity, and a characteristic radius of $80 \mu\text{m}$ ($1/e$). We measured the basic characteristics of a thulium MOT: the number, lifetime, and temperature of the atoms [33].

To determine the number of atoms in the MOT, we detected the luminescence of the cloud atoms excited by photons of the cooling beams. The luminescence signal was measured with a PMT operating in the current regime (see Fig. 2). The number of trapped atoms could be varied in the range from 10^2 to 10^7 , depending on the intensity and frequency detuning of cooling beams and the atomic beam intensity.

The dynamics of the number of atoms in the MOT is governed by the following equation [22]

$$\frac{dN}{dt} = R - \Gamma N - \beta N^2, \quad \beta = \frac{\sigma'}{2\sqrt{2}\pi^{1.5}r^3}, \quad (1)$$

where R is the atom trapping rate in the MOT, Γ is the linear loss coefficient (reciprocal to the lifetime), β is the quadratic loss coefficient, r is the cloud radius at the $1/e$ level, and $\sigma' = \langle v\sigma \rangle$ is the rate constant of binary atomic collisions. If the MOT loading is terminated at the instant of time $t = 0$ ($R_{t<0} \neq 0$, $R_{t>0} = 0$), the number of trapped atoms will decrease by the law

$$N(t) = \frac{N_0 \exp(-\Gamma t)}{1 + \beta N_0 \Gamma^{-1} [1 - \exp(-\Gamma t)]}. \quad (2)$$

In turn, the loading curve ($R_{t<0} = 0$, $R_{t>0} \neq 0$) will be described by the expression

$$N(t) = \frac{1}{2\beta} \left[-\gamma + \sqrt{\gamma^2 + 4\beta R} \tanh \left(\frac{t+c}{2} \sqrt{\gamma^2 + 4\beta R} \right) \right], \quad (3)$$

where c is the constant determined from the condition $N(0) = 0$. By neglecting binary collisions, expression (2) is simplified:

$$N(t) = N_0 \exp(-\Gamma t), \quad (4)$$

where N_0 is the initial number of atoms. Obviously, the loading process in this case will also be described by an exponential with the same time constant.

The linear loss coefficient comprises two terms: $\Gamma = \Gamma_0 + \Gamma_1$. The first term Γ_0 , related to collisions of atoms in the MOT with residual gas in the vacuum chamber, is independent of the cooling radiation intensity. The second term Γ_1 is related to the decay of the upper energy level of the cooling transition to other levels (see Fig. 1). This term depends on the upper-level population and, hence, on the intensity of cooling beams.

The exact solution to the problem requires the consideration of many intermediate atomic energy levels and unknown transition probabilities. By using theoretical estimates [11] predicting a small value of the branching ratio on the order of 10^{-5} , we considered the simplified two-level model in which an excited atom can irrevocably leave the cooling cycle with the probability $k\gamma$ (k is the unknown branching ratio). The linear loss coefficient in this model takes the form

$$\Gamma = \tau^{-1} = \Gamma_0 + \Gamma_1 \frac{N_2}{N} = \Gamma_0 + \frac{\Gamma_1}{2} \frac{S}{1 + S + 4\delta^2}, \quad (5)$$

where $S = I/I_{\text{sat}}$ is the saturation parameter, $I_{\text{sat}} = \pi\hbar c/3\lambda^3\tau = 18.9 \text{ mW cm}^{-2}$ is the transition saturation intensity (here, λ is the cooling transition wavelength, and τ is the upper-level lifetime), and δ stands for the detuning from the resonance in units of γ .

We determined the branching ratio by measuring the dependence of the lifetime τ on the intensity of cooling beams (the saturation parameter S). The measurements were performed for a relatively small number of trapped atoms (10^5) and the cloud radius of order $100 \mu\text{m}$. The experiments showed that binary atomic collisions under such conditions are insignificant [33], and simplified model (4) can be applied.

The lifetime was measured by the decay curve of the trap after switching off loading. The loading was terminated by switching off the Zeeman slower. The time dependence of luminescence of atoms in the MOT, detected with a PMT, was approximated by the model expression (4). Figure 4 presents the dependence of the lifetime of atoms in the MOT on the power of cooling beams for three values of the frequency detuning. By approximating the data using expression (5), we obtained the probability for the upper-level decay: $\Gamma_1 \geq 22(6) \text{ s}^{-1}$. The inequality sign appears here because a part of the population from intermediate atomic energy levels can return to the cooling cycle, and therefore we can give only the lower bound for Γ_1 . The branching ratio $k \geq 3.5 \times 10^{-7}$ corresponds to this value of Γ_1 , which does not contradict calculations [11].

As the concentration of atoms in the MOT increases, binary particle collisions begin to play a noticeable role. This is confirmed by the fact that the experimental unloading curve is already poorly described by approximate expression (4), and exact expression (2) should be used for trap unloading, and expression (3) for trap loading. Fitting curves at the concentration of atoms at the trap center equal to 10^{12} cm^{-3} are compared in the inset to Fig. 4.

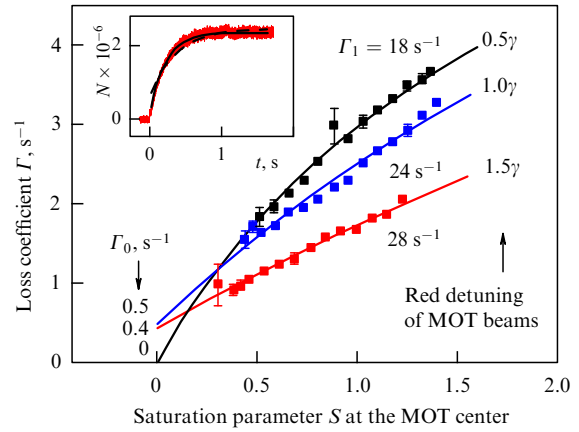


Figure 4. Dependences of the loss coefficient Γ on the cooling beam intensity for three red detunings. The data are approximated by expression (5). Measurements were performed for a small number of atoms in a trap (10^5) when the role of binary collisions is negligible. The inset shows the trap loading curve for a large number of atoms (2×10^6) in the MOT. The dashed curve is the exponential fit, and the solid curve is the fit by expression (3).

We estimated the rate constant of binary collisions of thulium atoms in the MOT as $\sigma' = 3(2) \times 10^{-10} \text{ cm}^3 \text{ s}^{-1}$. Collisions in the operating MOT occur between both ground-state and excited atoms, the cross sections for these collisions being considerably different. Nevertheless, the rate constant σ' is close to the value $10^{-10} \text{ cm}^3 \text{ s}^{-1}$ obtained in paper [12] where Tm–Tm collisions between spin-polarized ground-state atoms confined in a magnetic trap were studied.

4. Sub-Doppler cooling and a magnetic trap

4.1 Doppler and sub-Doppler cooling mechanisms

The final temperature that can be achieved upon laser cooling of atoms is determined by a balance between the cooling and heating rates, which appears during absorption and re-emission of cooling laser radiation. According to book [34], the Maxwell velocity distribution of atoms is formed in the stationary regime, which allows the use of such a parameter as the cloud temperature T .

Initially, the Doppler theory of laser cooling for a two-level atom was developed [35]. In the approximation of $I < I_{\text{sat}}$, the final temperature of cooled atoms in the Doppler theory depends on the red frequency detuning δ (in units of γ) of cooling radiation from the resonance as

$$T(\delta) = \frac{\hbar\gamma}{2k_B} \frac{\delta^2 + 1/4}{\delta}, \quad (6)$$

where k_B is the Boltzmann constant. This temperature has a minimum at $\delta = 1/2$, which is called the Doppler limit:

$$T_D = \frac{\hbar\gamma}{2k_B}. \quad (7)$$

For the 410.6-nm transition in a thulium atom, $T_D = 240 \mu\text{K}$. This temperature is too high for solving the problem of trapping atoms in an optical lattice or detailed studies of particle collisions in the quantum regime. The necessity appears to apply other methods to lower the temperature, for example, *sub-Doppler* cooling.

For atoms with the nondegenerate structure of magnetic sublevels in the ground state (in particular, ^{169}Tm), additional mechanisms are involved which cause the increase in cooling rate and temperature lowering [36]. The minimal temperature achieved by sub-Doppler cooling approaches the *recoil limit* $T_{\text{rec}} = h^2/(2\lambda^2 mk_B)$, which is usually considerably lower than the Doppler limit (m is the atomic mass). For the 410.6-nm transition in thulium, this limit is 330 nK.

For sub-Doppler cooling on $F \rightarrow F+1$ fine-structure transitions (F is the total momentum of the atom), the final atomic temperature depends on the detuning δ and light field intensity I as [37]

$$T \propto \frac{I}{F\delta}. \quad (8)$$

Unlike temperature (6) in the Doppler theory, which passes minimum (7), the atomic temperature in the sub-Doppler regime monotonically decreases upon increasing the frequency detuning δ .

The sub-Doppler cooling mechanism is very sensitive to a magnetic field [38–40]. In the absence of a magnetic field, the Doppler and sub-Doppler cooling mechanisms efficiently operate together. However, in the presence of a magnetic field B , the Doppler force is zero for atoms with the velocity

$$v_D = -g_e \frac{\mu_B B}{\hbar k}, \quad (9)$$

while the sub-Doppler force is zero for atoms with the velocity

$$v_S = -g_g \frac{\mu_B B}{\hbar k}, \quad (10)$$

where g_e and g_g are the Landé splitting factors for the upper and lower cooling levels, and k is the wave number. In this case, sub-Doppler cooling involves only a small velocity range around v_S . If velocities v_D and v_S considerably differ, only a small group of atoms are subjected to sub-Doppler cooling, which does not affect in fact the total cloud temperature. As the magnetic field is increased, the difference between velocities v_D and v_S also increases, which leads to the actual cessation of sub-Doppler cooling in alkali atoms already in magnetic fields of order 1 G [41].

This effect prevents the achievement of sub-Doppler temperatures directly in a MOT because, due to the finite size of the cloud and the adjustment inaccuracy, the cloud of cold atoms is collected not exactly at the zero point of the quadrupole magnetic field in the MOT. Because of this, a special cycle of sub-Doppler cooling is invoked in most experiments, when the quadrupole magnetic field in the MOT is switched off, the frequency detuning is increased, and the laser radiation intensity is decreased.

However, as follows from formulas (9) and (10), the efficient sub-Doppler cooling of atoms inside a MOT can be observed when the Landé g factors for the upper and lower cooling levels coincide [42]. For the 410.6-nm cooling transition in a thulium atom, the relative difference of g factors is only 2%, which provides efficient sub-Doppler cooling directly in the MOT.

4.2 Temperature of atoms in a magneto-optical trap

The cloud temperature was determined by the scattering of atoms after switching off the light and magnetic fields in a MOT (the ballistic scattering method). Within time Δt after switching off the fields, the cloud was illuminated by a short 200- μs probe laser pulse tuned exactly to the resonance of the

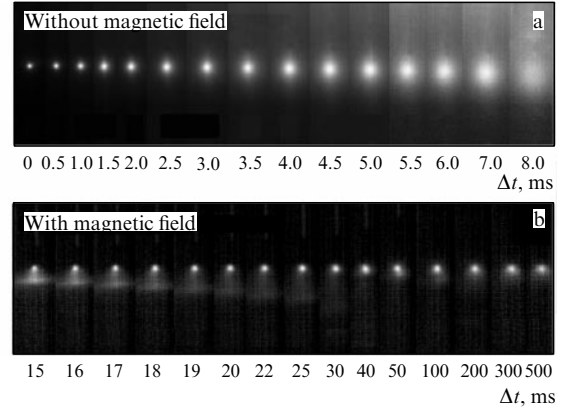


Figure 5. (a) Successive photographs of atoms flying apart in the ballistic regime in a MOT in the absence of a quadrupole magnetic field. The corresponding time intervals Δt are indicated in the figure. (b) Images of the cloud in a quadrupole magnetic field. The bright point shows magnetically trapped atoms; the elliptic cloud of untrapped atoms falling under the action of gravity is also observed.

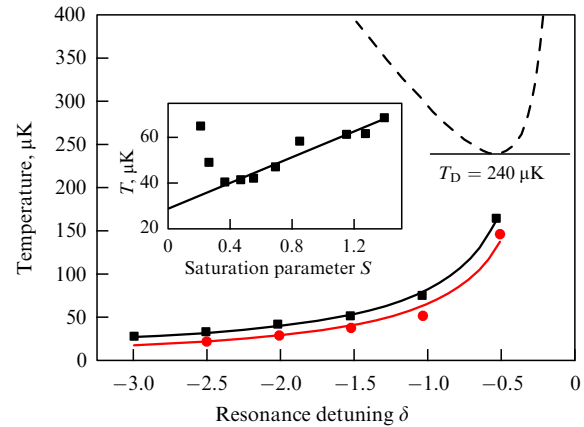


Figure 6. Dependence of temperature T on the frequency detuning δ of cooling radiation for radiation intensities $S = 2$ (squares) and 0.4 (circles). The dashed curve corresponds to the Doppler theory (6). The inset shows the dependence of temperature (squares) on the radiation intensity at the MOT center; the straight line is a linear fit of data for $S > 0.5$.

cooling transition (see Fig. 1). Photographs of the atomic cloud obtained within different time intervals after switching off the fields are presented in Fig. 5a.

Assuming the Maxwell velocity distribution of atoms, the dependence of the cloud radius r (at the $1/e$ level) on the delay time Δt takes the form

$$r(\Delta t) = \sqrt{r^2(0) + \frac{2k_B T}{m} \Delta t^2}. \quad (11)$$

Figure 6 depicts the dependence of the temperature of atoms on the frequency detuning of cooling beams, measured according to formula (11). The temperature decreases monotonically upon increasing the frequency detuning modulus, which suggests that sub-Doppler cooling dominates. For comparison, the dashed curve in Fig. 6 shows dependence (6) corresponding to the Doppler theory. As mentioned above, the high efficiency of sub-Doppler cooling in our case is determined by the close values of the Landé g_g and g_e factors of thulium energy levels involved in the cooling

process. The lowest detected temperature in the MOT was 25(5) μK .

The dependence of the temperature of atoms on the power of cooling beams is shown in the inset to Fig. 6. At low radiation intensities, the trap becomes unstable, resulting in the increase in temperature. At higher radiation powers, temperature increases linearly according to formula (8). The linear extrapolation leads to nonzero temperature at zero power, attesting the existence of an additional heating channel, which can be related to the inaccurate coincidence of the Landé g_e and g_g factors.

4.3 Magnetic trap

Ground-state thulium atoms possesses a large magnetic moment equal to $4\mu_B$. Due to the interaction of this moment with the quadrupole magnetic field of a MOT and due to low sub-Doppler temperatures in the latter, part of the atoms can be captured in a *magnetic trap* (MT). The atomic potential in such a trap is described by the expression

$$U(x, y, z) = \mu \sqrt{x^2 b_x^2 + y^2 b_y^2 + z^2 b_z^2} + mgz, \quad (12)$$

where μ is the effective magnetic moment of the atom, b_i is the magnetic field gradient along the i th axis, m is the atom mass, and g is the acceleration of gravity.

To study the MT, we performed experiments similar to temperature measurements, but with the switched-on quadrupole field of the MOT. Figure 5b gives a number of images recorded under such conditions. By comparing the atoms flying apart in the MOT in Figs 5a and 5b, we see that a fraction of the atoms from the MOT is confined in the MT for a long time, up to 0.5 s, whereas in the absence of the quadrupole field the atoms fly apart for about 10 ms. The photographs in Fig. 5b also show the image of atoms that are not confined in the magnetic trap and fall under the action of gravity.

The spatial profile of the MT is not Gaussian, and for this reason the temperature was estimated by the method described in paper [42]. Measurements give the temperature of atoms in the MT from 15 to 50 μK , depending on the initial temperature of atoms in the MOT. It is expected that the temperature of atoms in the MT should be approximately 1/3 of the temperature of atoms in the MOT [43], which is confirmed by experimental results.

5. The outlook

To study metrological characteristics of the 1.14- μm transition in a thulium atom and collisions of atoms in the quantum regime, we plan to load atoms into an optical dipole trap or an optical lattice. The second harmonic of a neodymium laser at 532 nm can be used as radiation for the optical trap. In this case, red detuning from the resonant 530.7-nm transition (see Fig. 1) and all other strong transitions in the blue spectral region is realized. Estimates show that for 2 W of radiation power and focusing to a waist 25 μm in radius, the trap depth corresponds to a temperature of 30 μK . The optical trap opens the possibility of studying collisions between atoms in different spin states, scattering cross sections in different magnetic fields (Feshbach resonances), and characteristics of the metrological transition discussed in Section 2. However, to perform reliable loading into the optical trap, it is desirable to achieve a temperature lower than 10 μK .

To reduce the temperature, we plan to realize the secondary cooling cycle on the weaker, completely cyclic 530.7-nm $4f^{13}6s^2 (J = 7/2) \rightarrow 4f^{12}5d_{5/2}6s^2 (J = 9/2)$ transition with a natural linewidth of 360 kHz (see Fig. 1). In so doing, the Doppler limit is reduced to 9 μK . Taking into account that the Landé g factors for the corresponding energy levels are also close, we expect a further decrease in temperature due to sub-Doppler mechanisms. This transition can be excited by the second harmonic of a frequency-stabilized semiconductor laser. Thus, we can anticipate the capture of a few million atoms at a temperature of order 1 μK , followed by their loading into an optical trap or lattice.

We also plan in parallel to construct a subhertz laser for exciting the 1.14- μm clock transition. The laser will be stabilized with respect to a vibration- and temperature-compensated resonator, as described in review [5]. The transition will be detected by a luminescence signal from the strong 410.6-nm transition, which is sensitive to the ground-state depopulation.

6. Conclusions

Analysis of the latest studies on the laser cooling of rare-earth atoms and the possibility of using them in precision spectroscopy and metrology and for studying their interactions in the quantum regime has shown that, due to the specific structure of the electron shells in Tm, the 1.14- μm magnetic dipole transition in a thulium atom can be of considerable interest for the development of a new optical clock with high short-term stability.

We have constructed a magneto-optical trap for thulium atoms and studied their laser cooling at a wavelength of 410.6 nm. The lifetime of atoms in the trap has been measured and the decay constant of the upper cooling level has been determined. It has been shown that, owing to the unique energy level diagram, sub-Doppler cooling is observed directly in the MOT without utilizing a special additional cycle. The lowest temperature achieved in the MOT is 25(5) μK for the number of atoms equal to 3×10^6 and the cloud radius of 80 μm , which corresponds to the phase density $\rho = 10^{-5}$.

Our studies have shown that the further cooling of thulium atoms to 1 μK is also possible, which is required for the loading of atoms into an optical trap or an optical lattice formed by a standing light wave.

Acknowledgments

The author expresses deep appreciation to all the participants in the project on laser cooling of thulium: V N Sorokin, S I Kanorsky, A V Akimov, A V Sokolov, K A Chebakov, and D D Sukachev, whose studies were used in this paper. Special thanks are due to G A Mesyats and A V Masalov for their constant support of the project.

This work was supported by DFG (grant No. 436Rus 113/984/0-1), the Presidential grant for young scientists, MD-669.2011, and the Program of Fundamental Studies: Extreme Light Fields and Their Applications, of the RAS Presidium.

References

1. Kolachevsky N N *Usp. Fiz. Nauk* **174** 1171 (2004) [*Phys. Usp.* **47** 1101 (2004)]
2. Chou C W et al. *Phys. Rev. Lett.* **104** 070802 (2010)

3. Cacciapiuoti L et al. *Nucl. Phys. B Proc. Suppl.* **166** 303 (2007)
4. Grosche G et al. *Opt. Lett.* **34** 2270 (2009)
5. Kolachevsky N N *Usp. Fiz. Nauk* **178** 1225 (2008) [*Phys. Usp.* **51** 1180 (2008)]
6. Blatt S et al. *Phys. Rev. Lett.* **100** 140801 (2008)
7. Aleksandrov E B et al. *Opt. Spektrosk.* **54** 3 (1983) [*Opt. Spectrosc.* **54** 1 (1983)]
8. Hancox C I et al. *Nature* **431** 281 (2004)
9. Chu X, Dalgarno A, Groenenboom G C *Phys. Rev. A* **75** 032723 (2007)
10. Buchachenko A A et al. *Phys. Scripta* **80** 048109 (2009)
11. Kolachevsky N et al. *Appl. Phys. B* **89** 589 (2007)
12. Connolly C B et al. *Phys. Rev. A* **81** 010702(R) (2010)
13. Ovsyannikov V D, Private discussions
14. Katori H et al. *Phys. Rev. Lett.* **91** 173005 (2003)
15. Ludlow A D et al. *Science* **319** 1805 (2008)
16. Melentiev P N et al. *Pis'ma Zh. Eksp. Teor. Fiz.* **83** 16 (2006) [*JETP Lett.* **83** 14 (2006)]
17. Goncharov A N et al., in *ICCNOLAT: Int. Conf. on Coherent and Nonlinear Optics, Int. Conf. on Lasers, Applications, and Technologies, Kazan, 23–26 August 2010*, IWB3 p. 74
18. Ryabtsev I I et al. *Phys. Rev. Lett.* **104** 073003 (2010)
19. Martiyanov K, Makhalov V, Turlapov A *Phys. Rev. Lett.* **105** 030404 (2010)
20. Domnin Y et al., in *Precise Time and Time Interval: 41st PTTI Meeting, Santa Ana Pueblo, New Mexico, November 16–19, 2009*
21. Riehle F *Frequency Standards: Basics and Applications* (Weinheim: Wiley-VCH, 2004) [Translated into Russian (Moscow: Fizmatlit, 2009)]
22. Weiner J et al. *Rev. Mod. Phys.* **71** 1 (1999)
23. Leggett A J *Rev. Mod. Phys.* **73** 307 (2001)
24. Hachisu H et al. *Phys. Rev. Lett.* **100** 053001 (2008)
25. Brickman K-A et al. *Phys. Rev. A* **76** 043411 (2007)
26. Andresen G B et al. *Nature* **468** 673 (2010)
27. Cano D et al. *Phys. Rev. Lett.* **101** 183006 (2008)
28. Stuhler J et al. *Phys. Rev. Lett.* **95** 150406 (2005)
29. Sawyer B C et al. *Phys. Rev. Lett.* **98** 253002 (2007)
30. McClelland J J, Hanssen J L *Phys. Rev. Lett.* **96** 143005 (2006)
31. Lu M, Youn S H, Lev B L *Phys. Rev. Lett.* **104** 063001 (2010)
32. Chebakov K et al. *Opt. Lett.* **34** 2955 (2009)
33. Sukachev D et al. *Phys. Rev. A* **82** 011405(R) (2010)
34. Minogin V G, Letokhov V S *Davlenie Lazernogo Izlucheniya na Atomy* (Laser Light Pressure on Atoms) (Moscow: Nauka, 1986) [Translated into English (New York: Gordon and Breach Science Publ., 1987)]
35. Letokhov V S, Minogin V G, Pavlik B D *Zh. Eksp. Teor. Fiz.* **72** 1328 (1977) [*Sov. Phys. JETP* **45** 698 (1977)]
36. Dalibard J, Cohen-Tannoudji C *J. Opt. Soc. Am. B* **6** 2023 (1989)
37. Chang S et al. *Phys. Rev. A* **64** 013404 (2001)
38. Valentin C et al. *Europhys. Lett.* **17** 133 (1992)
39. Shang S-Q et al. *Phys. Rev. Lett.* **67** 1094 (1991)
40. Walhout M et al. *J. Opt. Soc. Am. B* **9** 1997 (1992)
41. Walhout M, Sterr U, Rolston S L *Phys. Rev. A* **54** 2275 (1996)
42. Berglund A J, Lee S A, McClelland J J *Phys. Rev. A* **76** 053418 (2007)
43. Stuhler J et al. *Phys. Rev. A* **64** 031405(R) (2001)